4.2 Coastal upwelling fronts and jets.

(*A general reference to upwelling jets would be nice, perhaps Jack and Andy would know a good one. It could be cited after the first sentence below.)*

When the wind blows along a Northern Hemisphere coastline such that the coast lies left of the downwind direction, offshore Ekman transport is created at the surface. Water moves offshore and is replaced by deeper fluid that upwells and creates colder surface temperatures at the coast. A view of the resulting state as it would appear in a two-layer idealization is shown in Figure 4.2.1. The continental shelf is represented by a sloping region over which the total depth increases from zero to D_o. The shelf terminates in a vertical wall (nondimensionally $x=w$) that represents the continental slope. Offshore of this point the depth is infinite and the lower layer is inactive. The interface profile (I) shows the state that might occur before the upwelling event. As a result of the upwelling, lower layer fluid is brought up onto the shelf causing the interface to ground on the bottom (II) or to outcrop at the surface (III) or (IV). The sloping interface implies a cross-shelf pressure gradient and the latter tends to be balanced by an along-shore flow. In the northern hemisphere the upper layer flow runs with the coast on its left. Jet-like flows are observed along the northwest American coastline and along other coasts that experience upwelling.

Once a jet is established, it will experience topographic interactions due to capes, canyons, and other irregularities in the coastline. As shown in Figure 4.2.2, a southward flowing jet along the Oregon and Californian coastline passes several promontories, including Capes Blanco and Mendocino. The cool (darker) areas in the lees of these features represent deeper fluid that has welled up to the surface. In the context of Figure 1, these pools could be created when the interface evolves from profiles I or II, for which the interface grounds on the shelf, to (III) or (IV), where it outcrops at the surface. A number of investigators have attempted to explain these and other aspects of along-shore evolution using a hydraulic theory for the coastal jet. The descriptions below are based primarily on the work of Gill and Schumann (1979), who applied such a model to the Agulhas Current, and on Dale and Barth (2001), who applied a closely related model to Cape Blanco. A simplified version of the model was used by Stommel (1960, Chapter 8) to simulate the Gulf Stream along the eastern United States coastline.

The story just told tacitly ignores frictional effects, even though Ekman layer dynamics are essential to the upwelling. Nevertheless, it will be assumed that once the along-shore flow is set up, friction will not contribute significantly to evolution over limited regions of strong topographic variation. At the same time, we invoke the usual assumption of gradual along-shore variations in the coastal geometry, meaning that $w^*(y)$ varies on a scale large compared to w^* itself. The sea surface will be treated as a rigid lid and the shelf break depth D_o will be considered fixed. Capes are then represented as a narrowing of the shelf (a decrease in w^*), which is consistent with the bathymetry of the Oregon coast.

The dynamics of the upper layer involve interactions with the lower, a process that has not been explored thus far. Although a detailed development of this subject takes place in Section 5.1, the uninitiated reader should be able to follow this section with little need of help. The top and bottom layers will be numbered '1' and '2' respectively and, in accordance with the semigeostrophic approximation, the alongshore velocity components v_1* and v_2* will be considered geostrophic. The upper layer is assumed to be capped by a rigid lid and the pressure there is denoted by p_T*. The geostrophic relations for the two layers are then given by

$$fv_1^* = \frac{1}{\rho_1}\frac{\partial p_T^*}{\partial x^*} \tag{4.2.1}$$

and

$$fv_2^* = \frac{1}{\rho_1}\frac{\partial p_T^*}{\partial x^*} - g\frac{\partial d_1^*}{\partial x^*},$$

where d_1* is the upper layer thickness and g is the reduced gravity. The pressure gradient term on the right-hand side of the second equation follows from the hydrostatic relation. Subtraction of the second equation from the first results in the *thermal wind* relation

$$f(v_1^* - v_2^*) = g\frac{\partial d_1^*}{\partial x^*}. \tag{4.2.2}$$

The semigeostrophic potential vorticity of the upper layer will be considered constant:

$$\frac{f + \dfrac{\partial v_1^*}{\partial x^*}}{d_1^*} = \frac{f}{D_{1\infty}}, \tag{4.2.3}$$

even though there is little in the way of observation or deduction to justify the constancy of $D_{1\infty}$. The assumption is made purely for convenience. As for the lower layer potential vorticity:

$$\frac{f + \dfrac{\partial v_2^*}{\partial x^*}}{d_2^*} = \frac{f}{D_{2\infty}}, \tag{4.2.4}$$

it will be sufficient to assume that $D_{2\infty} >> D_{1\infty}$, as suggested by Figure 1, even though $D_{2\infty}$ need not be constant.

Let $D_{1\infty}$, $(gD_{1\infty})^{1/2}$, $\rho_1 gD_{1\infty}$, $(gD_{1\infty})^{1/2}/f$ and f^{-1} serve as scales for depth, alongshore velocity, rigid lid pressure, horizontal length, and time. Then (4.2.1)-(4.2.4) become

$$v_1 = \frac{\partial p_T}{\partial x} \tag{4.2.5}$$

$$1 + \frac{\partial v_1}{\partial x} = d_1, \tag{4.2.6}$$

$$1 + \frac{\partial v_2}{\partial x} = d_2 \frac{D_{1\infty}}{D_{2\infty}} << 1. \tag{4.2.7}$$

and

$$v_1 - v_2 = \frac{\partial d_1}{\partial x}. \tag{4.2.8}$$

Note that the approximation in (4.2.7) is valid only over the shelf, where lower layer fluid has risen up and where $D_{1\infty}$ is a legitimate scale for the lower layer depth. Offshore of the shelf break the constraint (4.2.8) is replaced by the condition v_2=0, in which case (4.2.6) and (4.2.8) yield

$$\frac{\partial^2 d_1}{\partial x^2} - d_1 = -1. \tag{4.2.9}$$

With the requirement that d_1 remain bounded as $x \to \infty$, the solution takes the form

$$d_1 = p_T = 1 + d(w, y, t)e^{-(x-w)}. \tag{4.2.10}$$

Over the shelf the solutions depend on the configuration (I), (II), (III), or (IV) of Figure 4.2.1. Where the upper layer occupies the whole water column, the velocity is computed from (4.2.6) with d_1 equal to the specified shelf depth. Where both layers are present, the solution is obtained by differentiating (4.2.8) with respect to x and using (4.2.6) and (4.2.7) to eliminate the derivatives of v_1 and v_2. The resulting equation for the upper layer depth is

$$\frac{\partial^2 d_1}{\partial x^2} - d_1 = 0. \tag{4.2.11}$$

Marching through the mathematics for all four configurations is rather tedious and we therefore limit a detailed discussion to case (II): the most difficult and most interesting of the four. Although the primary focus is on steady flow, the retention of time-dependence is not burdensome. Certain aspects of the nonlinear frontal or Kelvin

waves that arise are explored in the exercises at the end of the section. Hereafter we will assume that the shelf break depth d_o ($= D_o / D_{1\infty}$) is constant, so that

$$d_1 + d_2 = x d_o / w(y) \tag{4.2.12}$$

For Case (II), let $b(y,t)$ denote the x-position at which the interface grounds. Then the cross sectional structure of the flow in the various regions is given as follows. For the inshore region ($0 \le x \le b$):

$$v_1(x,y,t) = v_o + \frac{d_o x^2}{2w} - x \tag{4.2.13}$$

and

$$p_T(x,y,t) = p_o + v_o x + \frac{d_o x^3}{6w} - \frac{x^2}{2}, \tag{4.2.14}$$

where

$$v_o(y,t) = v_1(0,y,t) = e^{b-w} - \frac{d_o b}{w}\left(1 + \frac{b}{2}\right) + w \tag{4.2.15}$$

and

$$p_o = p_T(0,y,t) = -\tfrac{1}{2}w^2 - be^{b-w} + \frac{d_o b}{w}\left(1 + b + \frac{b^2}{3}\right). \tag{4.2.16}$$

The latter follows from the nondimensional geostrophic relation $v_1 = \partial p_T / \partial x$ for the upper layer.

For the shelf region occupied by both layers ($b \le x \le w$):

$$d_1(x,y,t) = \tfrac{1}{2}e^{x-w}(1 - e^{2(b-x)}) + \frac{d_o b}{w}e^{b-x}, \tag{4.2.17}$$

$$v_1(x,y,t) = \tfrac{1}{2}e^{x-w}(1 + e^{2(b-x)}) - \frac{d_o b}{w}e^{b-w} + w - x, \tag{4.2.18}$$

and

$$p_T(x,y,t) = d_1(x,y,t) - \tfrac{1}{2}(x-w)^2. \tag{4.2.19}$$

Finally, the offshore region ($x \ge w$) has

$$v_1(x,y,t) = \tfrac{1}{2}e^{w-x}(1 + e^{2(b-w)}) - \frac{d_o b}{w}e^{b-x} \tag{4.2.20}$$

and

$$p_T(x,y,t) = d_1(x,y,t) = 1 - v_1(x,y,t)\,. \tag{4.2.21}$$

The coefficients in the above expressions have been chosen such that p_T and v_1 are continuous across the boundaries $x=b$ and $x=w$ of the three regions. These requirements ensure that d_1 will also be continuous.

The y-momentum equation for the upper layer can be used to calculate the behavior of the along-shore current in y and t. A convenient form to use is

$$\frac{\partial v_1}{\partial t} + \left(1 + \frac{\partial v_1}{\partial x}\right) u_1 = -\frac{\partial}{\partial y}\left(p_T + \frac{v_1^{\,2}}{2}\right). \tag{4.2.22}$$

The second term, which is just $d_1 u_1$ times the upper layer potential vorticity, goes to zero at the coastline ($x=0$). Substitution of the expressions for v_1 and p_T (see 4.2.13-4.2.16) into this equation and evaluation of the result at $x=0$ leads to

$$\frac{\partial v_o}{\partial t} + \frac{\partial}{\partial y}\left(B_o\right) = 0\,, \tag{4.2.23}$$

where B_o is the upper layer Bernoulli function at the coast:

$$B_o = \tfrac{1}{2} v_o^2(b,w) + p_o(b,w)\,, \tag{4.2.24}$$

with v_o and p_o given by (4.2.15) and (4.2.16).

Since all the time dependence is contained in the variable $b(y,t)$, while all the y-dependence is contained in b and w, (4.2.23) can be written in the form

$$\frac{\partial v_o}{\partial b}\frac{\partial b}{\partial t} + \frac{\partial B_o}{\partial b}\frac{\partial b}{\partial y} = -\frac{\partial B_o}{\partial w}\frac{\partial w}{\partial y},$$

or

$$\frac{\partial b}{\partial t} + c\frac{\partial b}{\partial y} = -\frac{\partial B_o}{\partial w}\frac{\partial w}{\partial y}\left(\frac{\partial v_o}{\partial b}\right)^{-1}, \tag{4.2.25}$$

where

$$c(b,w) = \frac{\partial B_o}{\partial b}\left(\frac{\partial v_o}{\partial b}\right)^{-1}. \tag{4.2.26}$$

It can be shown that the signal that propagates at speed $c(b,w)$ is essentially a Kelvin wave that has been modified by the presence of the current and the sloping bottom. Since the model admits just one wave, the concepts of subcritical or supercritical flow need to be rethought. The usual practice is to call the flow *supercritical* when the wave propagates in the same direction as the upper layer transport. The nominal direction of upper layer transport will be positive (with the northern hemisphere coastline on the left) and therefore supercritical and subcritical flow will be characterized by $c>0$ and $c<0$. In the latter case the wave propagates with the coast on its right; that is, in the usual sense for northern hemisphere Kelvin waves. There will also be some cases with negative upper layer transport, making the classification of the flow less straightforward.

We are now in a position to discuss case II steady solutions and their hydraulic properties. However, it will be helpful to first describe the properties of cases (I), (III), and (IV), which will be stated without proof. The reader who has mastered Sections 2.2 and 2.3 will not be surprised by most of what comes next. For case (I), the interface grounds along the vertical wall and the wave dynamics are similar to those of a Kelvin wave that propagates along the left wall of a wide channel (see Figure 2.3). Most importantly, the wave speed is negative regardless of the direction of the upper layer flux (cf. equation 2.2.26). Case (I) flows are therefore always subcritical. In Case (IV) the interface outcrops at a position offshore of the shelf break and the wave dynamics are identical to those that occur when the Figure 2.3 channel flow separates from the left wall. The characteristic wave speed is zero and the flow is exactly critical. The flow no longer feels the coastal topography and is essentially unforced. Case (III) is more difficult to describe in terms of previous results, but it can be shown that the wave speed is always positive and thus the flow is always supercritical (see exercise 3). Transitions between subcritical and supercritical flow can only occur when the interface grounds on the shelf (case II).

Under conditions of steady flow, B_o is a constant prescribed by upstream conditions. Solutions in this case could, in principle, be computed from (4.2.24). A useful alternative to this relation can be derived by first noting that

$$\partial B_1 / \partial x = v_1 \partial v_1 / \partial x + \partial p_T / \partial x = v_1(\partial v_1 / \partial x + 1) = v_1 d_1 .$$

The upper layer volume transport may therefore be written as

$$Q_1 = \int_0^\infty (v_1 d_1) dx = B_\infty - B_o(y,t)$$

where B_∞ is the is the value of the upper layer Bernoulli function at $y \to \infty$ and is equal to unity. Equation (4.2.24) can therefore be expressed as

$$\tfrac{1}{2} v_o^2(b,w) + p_o(b,w) = 1 - Q_1 . \qquad (4.2.27)$$

A set of steady solution curves for various values of Q_1, showing the interface outcrop position as a function of the shelf width appears in Figure 4.2.3. In order to present all cases with a single figure, the composite variable

$$\alpha = \begin{cases} b' & \text{(case III)} \\ -b & \text{(case II)} \\ -wd_1^+ / d_b & \text{(case I)} \end{cases} \qquad (4.2.28)$$

has been introduced. Recall that b or b' denotes the position of the inshore edge of the interface over the shelf (Figure 4.2.1). The shelf edge depth d_o=2 in all cases, and this means that the upper layer thickness far offshore (=1) is less.

Critical states in Figure 4.2.3 lie along the dashed curve that passes through the minima of the family of Q=constant curves. Subcritical flows lie to the left and correspond to instances of cases (I) or (II), whereas supercritical flows lie to the right and correspond to (II) or (III). Note that the slope of the all the curves for case (III) equals unity ($w=\alpha+const.$) and thus a solution with a surface outcrop over the shelf maintains a fixed distance w-α from the shelf edge. Case (IV) occurs along the line $\alpha=w$ (or Q=0.5); when the interface outcrops at the surface and this position is at or offshore of the shelf break, the flow is no longer forced by topographic variations.

A flow that is subcritical upstream may undergo a transition to supercritical flow due to a narrowing of the shelf. This evolution can be traced by following one of the constant Q curves from the left hand portion of the figure, though the minimum in w, and onto the right-hand branch. As this occurs, the inshore termination of the interface continuously rises along the shelf, possibly striking the surface and exposing the cold lower layer. There are also some features that complicate this traditional picture; one is that some of the curves have negative Q. The latter terminate at the origin and can therefore be joined with a subcritical solution branch only if the shelf width w goes to zero. Another complication is that for other values of d_b the solutions cannot always be continued smoothly through the subcritical regime. Dale and Barth (2001) should be consulted for further details.

Another view of the critically controlled solution appears in Figure 4.2.4, which is calculated using a more general model containing an approximation to the Cape Blanco topography. The dashed line in Figure 4.2.4b shows the position at which the interface grounds over the shelf and this curve turns solid where the grounding becomes a surface outcrop. Lower layer fluid is exposed along the coast to the south of this transition. Whether this accounts for the observed behavior of the front near Cape Blanco is unsettled; other explanations such as local enhancement of the winds by the Cape have also been put forward (e.g. Samelson et al., 2002).

Further results on time-dependent features of upwelling fronts can be found in the literature. Gill and Schumann (1979) discuss the nonlinear properties of the coastal

trapped waves that arise in all three cases. Some of these properties are drawn out in exercise 3 below. Dale and Barth (2001) describe some initial-value experiments that demonstrate blocking of the upstream flow by the cape.

Since the model discussed above is constrained to have uniform potential vorticity in each of the two layers, potential vorticity waves have been expunged. Among this group is the continental shelf wave which, in the absence of a background flow, propagates in the same direction as a Kelvin wave. Coastal flows with potential vorticity gradients may exhibit hydraulic behavior, though field examples have yet to be clearly identified. Hughes (1985a,b;1986a,b;1987) describes a variety of models, some of which will be touched on in Section 6.2. Particularly relevant to the present discussion is the (1985b) model, which allows for potential vorticity and Kelvin wave dynamics and shows that hydraulic transitions with respect to both are possible.

Exercises

1) Calculate the lower layer velocity over the shelf for case (II).

2) Calculate the characteristic wave speed for case II explicitly. Consider an initial condition in which b increases monotonically from one constant value to another. Discuss the direction of propagation of the resulting wave and the tendency to steepen or rarefy.

3) *The dynamics of Case* III.

(a) Show that the upper-layer, cross-shelf structure for case III is given by:

$$v_1(x,y,t) = \tfrac{1}{2} e^{w-x}(1+e^{2(b'-w)}) \text{ and}$$
$$p_T(x) = d_1(x) = 1 - v_1(x)$$

for $x>w$, and by

$$v_1(x,y,t) = \tfrac{1}{2} e^{w-x}(1+e^{2(b'-w)}) + w - x$$
$$p_T(x,y,t) = \tfrac{1}{2}[e^{w-x}(1-e^{2(b'-w)}) - (x-w)^2] \text{ and}$$
$$d_1(x,y,t) = \tfrac{1}{2} e^{w-x}(1-e^{2(b'-w)})$$

for $b' \le x \le w$. Note that b' is the position of the surface outcrop.

(b) To find the evolution of the flow in x and t, consider the y-momentum equation applied at the outcrop $x=b'$. A particularly convenient form of this equation is obtained by applying it *along* the outcrop, so that derivatives in y and t are taken *after* x is set to b in the expressions appearing in (a). To achieve this form first show that

$$\left(\frac{\partial}{\partial t}v(x,y,t)\right)_{x=b} = \frac{\partial}{\partial t}v(b'(x,t),y,t) - \left(\frac{\partial v(x,y,t)}{\partial x}\right)_{x=b}\frac{\partial b'(y,t)}{\partial t}$$

for any variable v. Show that a similar expression holds for y-derivatives. Now use expressions like this to replace local y- and t- derivatives in the upper layer y-momentum equation by derivatives of quantities first evaluated at $x=b'$. With the help of the geostrophic relation for v_1 and the potential vorticity definition, you should obtain

$$\frac{\partial}{\partial t}\left(v_1(b'(y,t),y,t)+b'(y,t)\right)+\frac{\partial}{\partial y}\left(p_T(b'(y,t),y,t)+\frac{v_1^2(b'(y,t),y,t)}{2}\right)=0\,.$$

Finally, apply this equation to the expressions derived in part (a) to obtain an evolution equation for b'. Identify the characteristic wave speed and show that it is non-negative.

(c) Show that for steady flow, b'-w remains conserved.

Figure Captions/Info

4.2.1 Definition sketch.

4.2.2 Sea surface temperature from May 18th 1995 at 21:00 UCT for a region of the US west coast. Isobaths are shown at 200m (approximates the shelf edge), 1000m, 2000m and 3000m. (Dale and Barth, 2001, Figure 1)

4.2.3 Solutions curves relating the shelf width w and position of interface outcrop α (see Equation 4.2.28) for various values of the upper layer transort Q_1. The shelf break depth d_o=2 in all cases. The figure is based on solutions to (4.2.27) for case II and the relations that govern steady flows in the remaining cases as they appear in Dale and Barth (2001). (Dale and Barth, 2001, Figure 7.)

4.2.4 Fields of (a) streamfunction and (b) upper layer thickness d_1 for approximated Cape Blanco topography. The solution shown is critically controlled and has Q=0.701. A dashed bold line shows the position $x=b$ where the interface grounds on the bed, and this turn to a solid bold line where the interface outcrops at the surface. (Dale and Barth 2001, Figure 13.)

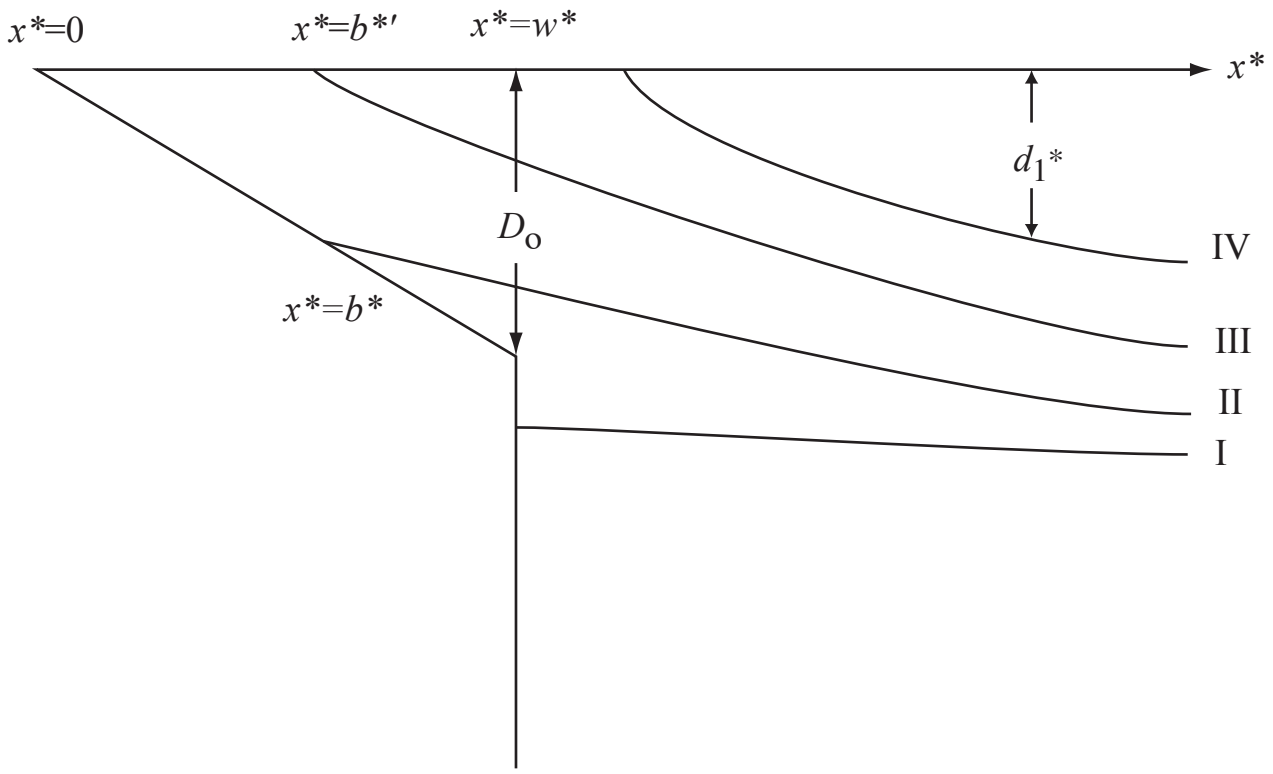

Figure 4.2.1

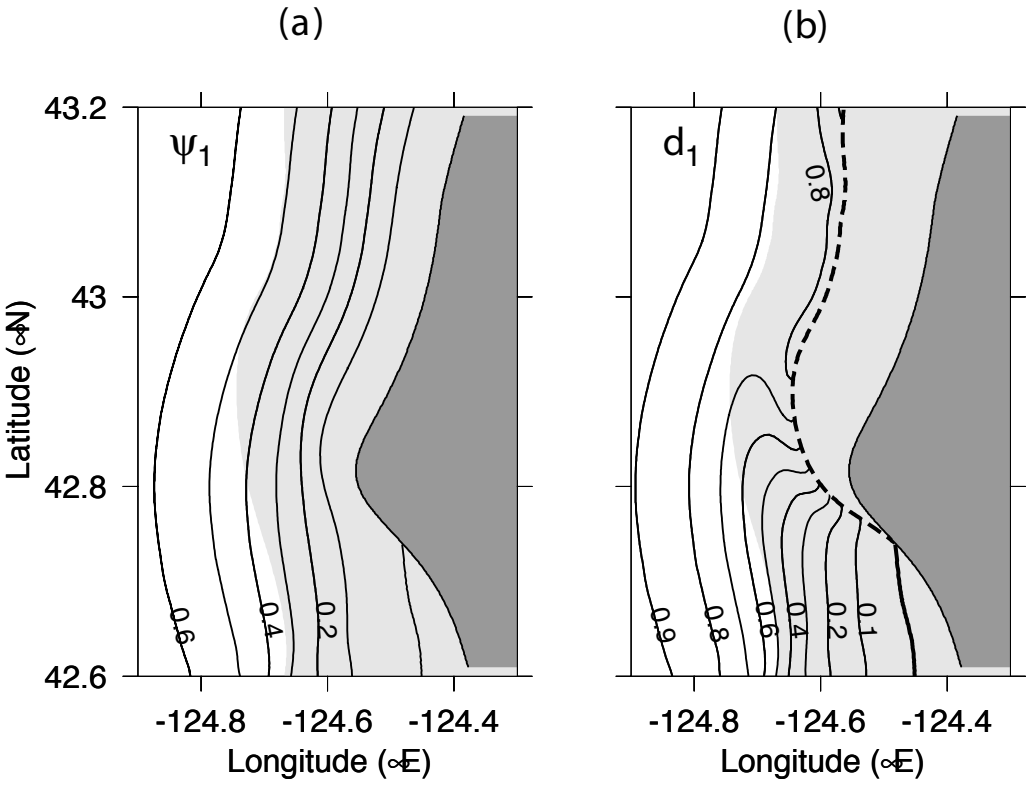
(a)
(b)
43.2
43
42.8
42.6
Latitude (°N)
ψ1
d1
0.6
0.4
0.2
0.8
0.9
0.8
0.6
0.4
0.2
0.1
-124.8
-124.6
-124.4
Longitude (°E)
-124.8
-124.6
-124.4
Longitude (°E)

Figure 4.2.4

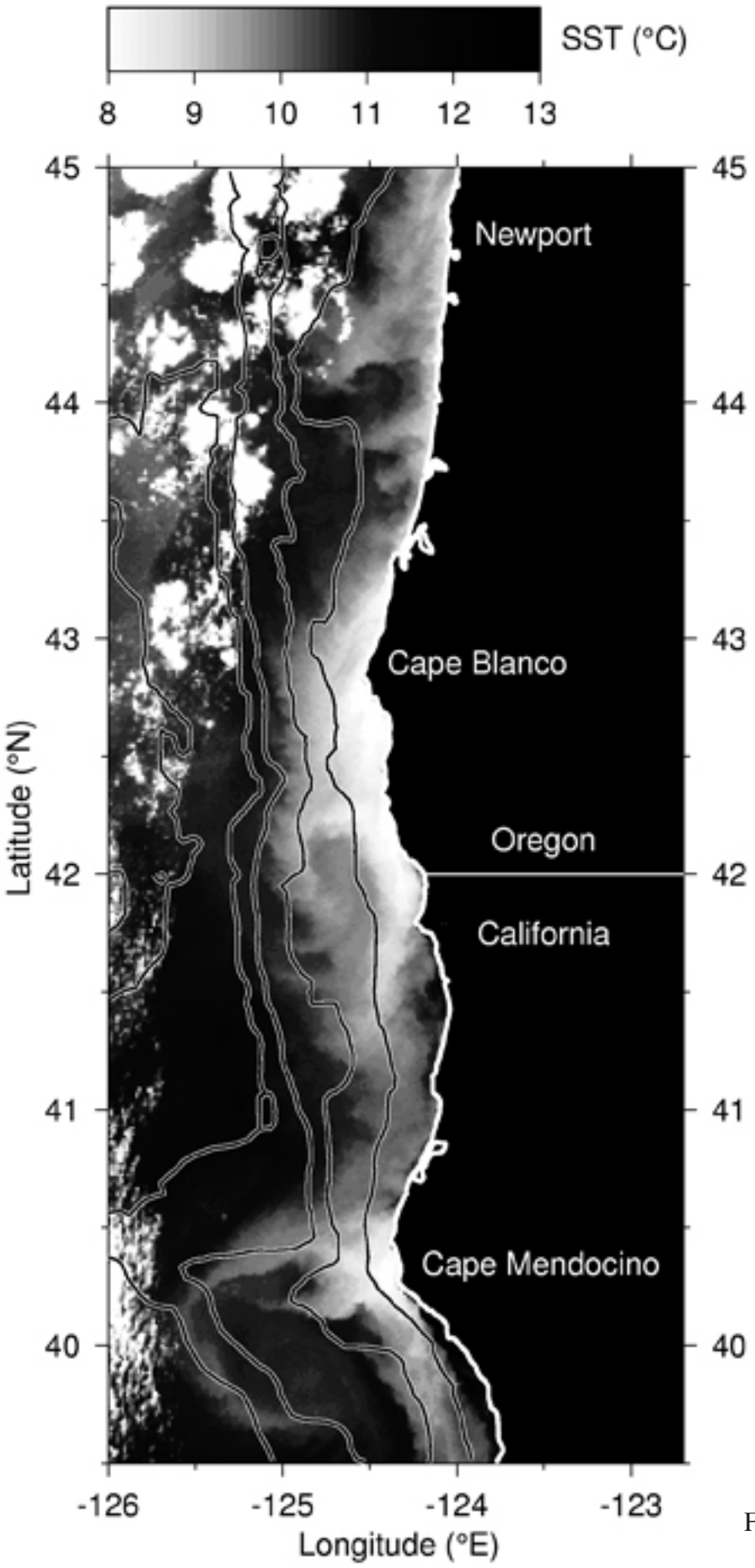
SST (°C)
8
9
10
11
12
13
45
44
43
42
41
40
Newport
Cape Blanco
Oregon
California
Cape Mendocino
Latitude (°N)
-126
-125
-124
-123
Longitude (°E)

Figure 4.2.2

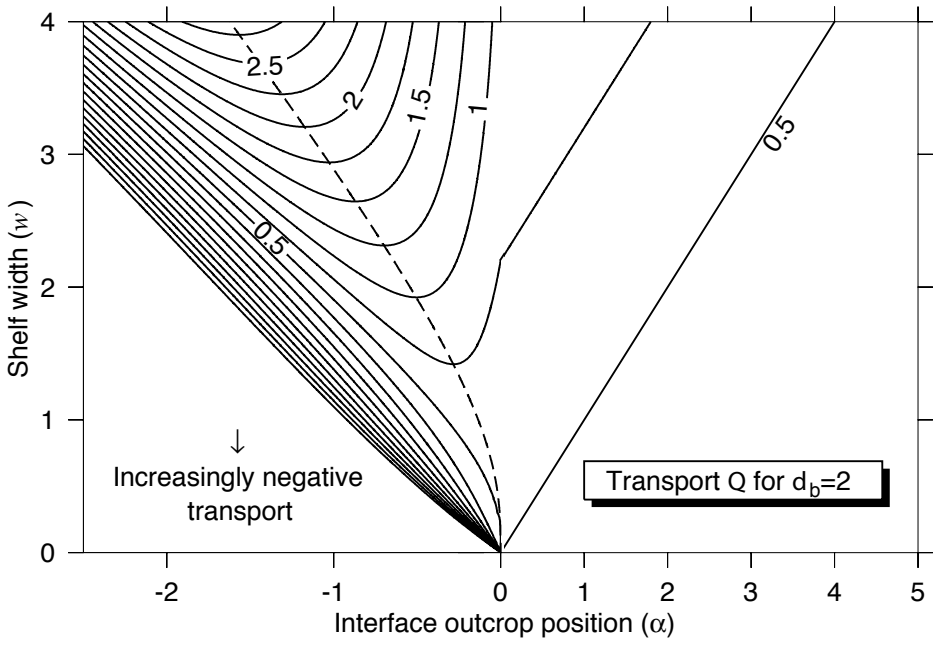
Shelf width (w)
Interface outcrop position (α)
2.5
2
1.5
1
0.5
0.5
Increasingly negative transport
Transport Q for d_b=2
0
1
2
3
4
-2
-1
0
1
2
3
4
5

Figure 4.2.3